Transiting hot Jupiters from WASP-South, Euler and TRAPPIST: WASP-95b to WASP-101b

Coel Hellier[1], D.R. Anderson[1], A. Collier Cameron[2], L. Delrez[3], M. Gillon[3],
E. Jehin[3], M. Lendl[4], P.F.L. Maxted[1], F. Pepe[4], D. Pollacco[5], D. Queloz[4,6],
D. Ségransan[4], B. Smalley[1], A.M.S. Smith[1,7], J. Southworth[1],
A.H.M.J. Triaud[4,8*], S. Udry[4] & R.G. West[5]

[1] *Astrophysics Group, Keele University, Staffordshire, ST5 5BG, UK*
[2] *SUPA, School of Physics and Astronomy, University of St. Andrews, North Haugh, Fife, KY16 9SS, UK*
[3] *Institut d'Astrophysique et de Géophysique, Université de Liège, Allée du 6 Août, 17, Bat. B5C, Liège 1, Belgium*
[4] *Observatoire astronomique de l'Université de Genève 51 ch. des Maillettes, 1290 Sauverny, Switzerland*
[5] *Department of Physics, University of Warwick, Gibbet Hill Road, Coventry CV4 7AL, UK*
[6] *Cavendish Laboratory, J J Thomson Avenue, Cambridge, CB3 0HE, UK*
[7] *N. Copernicus Astronomical Centre, Polish Academy of Sciences, Bartycka 18, 00-716 Warsaw, Poland*
[8] *Department of Physics and Kavli Institute for Astrophysics & Space Research, Massachusetts Institute of Technology, Cambridge, MA 02139, USA*

date

ABSTRACT

We report the discovery of the transiting exoplanets WASP-95b, WASP-96b, WASP-97b, WASP-98b, WASP-99b, WASP-100b and WASP-101b. All are hot Jupiters with orbital periods in the range 2.1 to 5.7 d, masses of 0.5 to 2.8 M_{Jup}, and radii of 1.1 to 1.4 R_{Jup}. The orbits of all the planets are compatible with zero eccentricity. WASP-99b shows the shallowest transit yet found by WASP-South, at 0.4%.

The host stars are of spectral type F2 to G8. Five have metallicities of [Fe/H] from –0.03 to +0.23, while WASP-98 has a metallicity of –0.60, exceptionally low for a star with a transiting exoplanet. Five of the host stars are brighter than $V = 10.8$, which significantly extends the number of bright transiting systems available for follow-up studies. WASP-95 shows a possible rotational modulation at a period of 20.7 d.

We discuss the completeness of WASP survey techniques by comparing to the HAT project.

Key words: planetary systems

1 INTRODUCTION

The WASP-South survey has dominated the discovery of transiting hot-Jupiter exoplanets in the Southern hemisphere. WASP-South is well matched to the capabilities of the Euler/CORALIE spectrograph and the robotic TRAPPIST telescope, with the combination of all three proving efficient for discovering transiting exoplanets in the range $V = 9$–13.

WASP-South has now been running nearly continuously for 7 years. Approximately 1000 candidates have been observed with Euler/CORALIE, while, since December 2010, TRAPPIST has observed 1000 lightcurves of WASP candidates and planets. Here we present new WASP-South planets which take WASP numbering above 100.

Since WASP host stars are generally brighter than host stars of *Kepler* exoplanets, ongoing WASP-South discoveries are important for detailed study of exoplanets and will be prime targets for future missions such as *CHEOPS* and *JWST*, and proposed missions such as *EChO* and *FINESSE*.

2 OBSERVATIONS

The observational and analysis techniques used here are the same as in recent WASP discovery papers (e.g. Hellier et al. 2012), and thus are described briefly. For detailed accounts see the early papers including Pollacco et al. (2006), Collier-Cameron et al. (2007a) and Pollacco et al. (2007).

In outline, WASP-South surveys the visible sky each

---

* Fellow of the Swiss National Science Foundation

Table 1. Observations

Facility	Date	
WASP-95:		
WASP-South	2010 May–2011 Nov	23 200 points
Euler/CORALIE	2012 Jul–2013 May	14 radial velocities
TRAPPIST	2012 Sep 14	z band
EulerCAM	2012 Sep 16	Gunn r filter
TRAPPIST	2012 Sep 27	z band
EulerCAM	2013 May 23	Gunn r filter
EulerCAM	2013 Aug 01	Gunn r filter
WASP-96:		
WASP-South	2010 Jun–2011 Dec	13 100 points
Euler/CORALIE	2011 Oct–2012 Oct	21 radial velocities
TRAPPIST	2011 Nov 11	Blue-block filter
EulerCAM	2012 Jul 01	Gunn r filter
TRAPPIST	2012 Dec 11	Blue-block filter
EulerCAM	2013 Jun 29	Gunn r filter
WASP-97:		
WASP-South	2010 Jun–2012 Jan	23 900 points
Euler/CORALIE	2012 Sep–2012 Nov	12 radial velocities
EulerCAM	2012 Nov 23	Gunn r filter
TRAPPIST	2012 Nov 23	z-band
EulerCAM	2013 Jul 11	Gunn r filter
EulerCAM	2013 Aug 09	Gunn r filter
TRAPPIST	2013 Aug 09	$I + z$ filter
WASP-98:		
WASP-South	2006 Aug–2012 Jan	12 700 points
Euler/CORALIE	2011 Nov–2012 Nov	15 radial velocities
EulerCAM	2012 Oct 28	$I_{\rm C}$ band
TRAPPIST	2012 Oct 28	blue-block filter
EulerCAM	2012 Oct 31	$I_{\rm C}$ band
TRAPPIST	2012 Nov 03	blue-block filter
TRAPPIST	2013 Aug 29	blue-block filter
EulerCAM	2013 Sep 07	$I_{\rm C}$ band
WASP-99:		
WASP-South	2010 Jul–2012 Jan	9000 points
Euler/CORALIE	2012 Feb–2013 Jan	20 radial velocities
EulerCAM	2012 Nov 21	Gunn r filter
WASP-100:		
WASP-South	2010 Aug–2012 Jan	13 500 points
Euler/CORALIE	2012 Sep–2013 Mar	19 radial velocities
TRAPPIST	2012 Dec 04	$I + z$ filter
TRAPPIST	2013 Jan 10	$I + z$ filter
TRAPPIST	2013 Sep 29	z filter
WASP-101:		
WASP-South	2009 Jan–2012 Mar	16 100 points
Euler/CORALIE	2011 Jan–2013 Jun	21 radial velocities
TRAPPIST	2012 Jan 11	z band
TRAPPIST	2012 Jan 22	z band
TRAPPIST	2012 Jan 29	z band
TRAPPIST	2012 Mar 05	z band
EulerCAM	2012 Dec 06	Gunn r filter
TRAPPIST	2013 Feb 23	z band

clear night using an array of 200mm f/1.8 lenses and a cadence of ~ 10 mins. Transit searching of accumulated lightcurves leads to candidates that are passed to TRAP-PIST (Jehin et al. 2011), a robotic 0.6-m photometric telescope, which can resolve blends and check that the candidate transits are planet-like, and to the 1.2-m Euler/CORALIE spectrograph, for radial-velocity observations. About 1 in 12 candidates turns out to be a planet. Higher-quality transit

lightcurves are then obtained with TRAPPIST and Euler-CAM (Lendl et al. 2012). A list of the observations reported here is given in Table 1 while the CORALIE radial velocities are listed in Table A1.

3   THE HOST STARS

For each star, the individual CORALIE spectra were co-added to produce a single spectrum with typical S/N of $\sim 100{:}1$ (though the fainter WASP-98, $V = 13$, had a S/N of only 40:1). Our methods for spectral analysis are described in Doyle et al. (2013). The excitation balance of the Fe I lines was used to determine the effective temperature ($T_{\rm eff}$), and spectral type was estimated from $T_{\rm eff}$ using the table in Gray (2008). The surface gravity ($\log g$) was determined from the ionisation balance of Fe I and Fe II. The Ca I line at 6439Å and the Na I D lines were also used as $\log g$ diagnostics. The metallicity was determined from equivalent width measurements of several unblended lines.

The projected stellar rotation velocity ($v \sin i$) was determined by fitting the profiles of several unblended Fe I lines. An instrumental FWHM of 0.11 ± 0.01 Å was determined from the telluric lines around 6300Å.

For age estimates we use the lithium abundance and the Sestito & Randlich (2005) calibration. We also give a gyrochronological age, from the measured $v \sin i$ and assuming that the star's spin is perpendicular to us, so that this is the true equatorial speed. This is then combined with the stellar radius to give a rotational period, to compare with the results of Barnes (2007). The results for each star are listed in the Tables 2 to 10. We also list proper motions from the UCAC4 catalogue of Zacharias et al. (2013). The motions and metallicities are all compatible with the stars being local thin-disc stars.

We searched the WASP photometry of each star for rotational modulations by using a sine-wave fitting algorithm as described by Maxted et al. (2011). We estimated the significance of periodicities by subtracting the fitted transit lightcurve and then repeatedly and randomly permuting the nights of observation. We found a marginally significant modulation in WASP-95 (see Section 4.2) but not in any of the other stars (with 95%-confidence upper limits being typically 1 mmag).

4   SYSTEM PARAMETERS

The CORALIE radial-velocity measurements were combined with the WASP, EulerCAM and TRAPPIST photometry in a simultaneous Markov-chain Monte-Carlo (MCMC) analysis to find the system parameters. For details of our methods see Collier Cameron et al. (2007b). The limb-darkening parameters are noted in each Table, and are taken from the 4-parameter non-linear law of Claret (2000).

For all of our planets the data are compatible with zero eccentricity and hence we imposed a circular orbit (see Anderson et al. 2012 for the rationale for this). The upper limits on the eccentricity range from 0.02 (for the $V = 9.5$ WASP-99) to 0.27 (for the fainter, $V = 12.2$, WASP-96).

Table 2. System parameters for WASP-95.

1SWASP J222949.73–480011.0
2MASS 22294972–4800111
RA = $22^h 29^m 49.73^s$, Dec = $-48°00'11.0''$ (J2000)
V mag = 10.1
Rotational modulation   2 mmag at ~ 20.7 d
pm (RA) 94.1 ± 0.9 (Dec) -8.5 ± 1.0 mas/yr

Stellar parameters from spectroscopic analysis.

Spectral type	G2
T_{eff} (K)	5830 ± 140
$\log g$	4.36 ± 0.07
$v \sin I$ (km s^{-1})	3.1 ± 0.6
[Fe/H]	$+0.14 \pm 0.16$
$\log A(Li)$	<0.2
Age (Lithium) [Gy]	>3
Age (Gyro) [Gy]	$2.4^{+1.7}_{-1.0}$

Parameters from MCMC analysis.

P (d)	2.1846730 ± 0.0000014
T_c (HJD) (UTC)	$245\ 6338.45851 \pm 0.00024$
T_{14} (d)	0.116 ± 0.001
$T_{12} = T_{34}$ (d)	0.011 ± 0.001
$\Delta F = R_P^2/R_*^2$	0.0105 ± 0.0003
b	$0.19^{+0.21}_{-0.13}$
i (°)	$88.4^{+1.2}_{-2.1}$
K_1 (km s^{-1})	0.1757 ± 0.0017
γ (km s^{-1})	6.2845 ± 0.0004
e	0 (adopted) (<0.04 at 3σ)
M_* (M$_\odot$)	1.11 ± 0.09
R_* (R$_\odot$)	$1.13^{+0.08}_{-0.04}$
$\log g_*$ (cgs)	$4.38^{+0.02}_{-0.04}$
ρ_* ($\rho_\odot$)	$0.78^{+0.04}_{-0.13}$
T_{eff} (K)	5630 ± 130
M_P (M$_{Jup}$)	$1.13^{+0.1}_{-0.04}$
R_P (R$_{Jup}$)	1.21 ± 0.06
$\log g_P$ (cgs)	$3.34^{+0.02}_{-0.07}$
ρ_P (ρ_J)	$0.85^{+0..07}_{-0.2}$
a (AU)	0.03416 ± 0.00083
$T_{P,A=0}$ (K)	1570 ± 50

Errors are 1σ; Limb-darkening coefficients were:
(Euler r) a1 = 0.701, a2 = –0.490, a3 = 1.077, a4 = –0.516
(Trap z) a1 = 0.780, a2 = –0.718, a3 = 1.082, a4 = –0.487
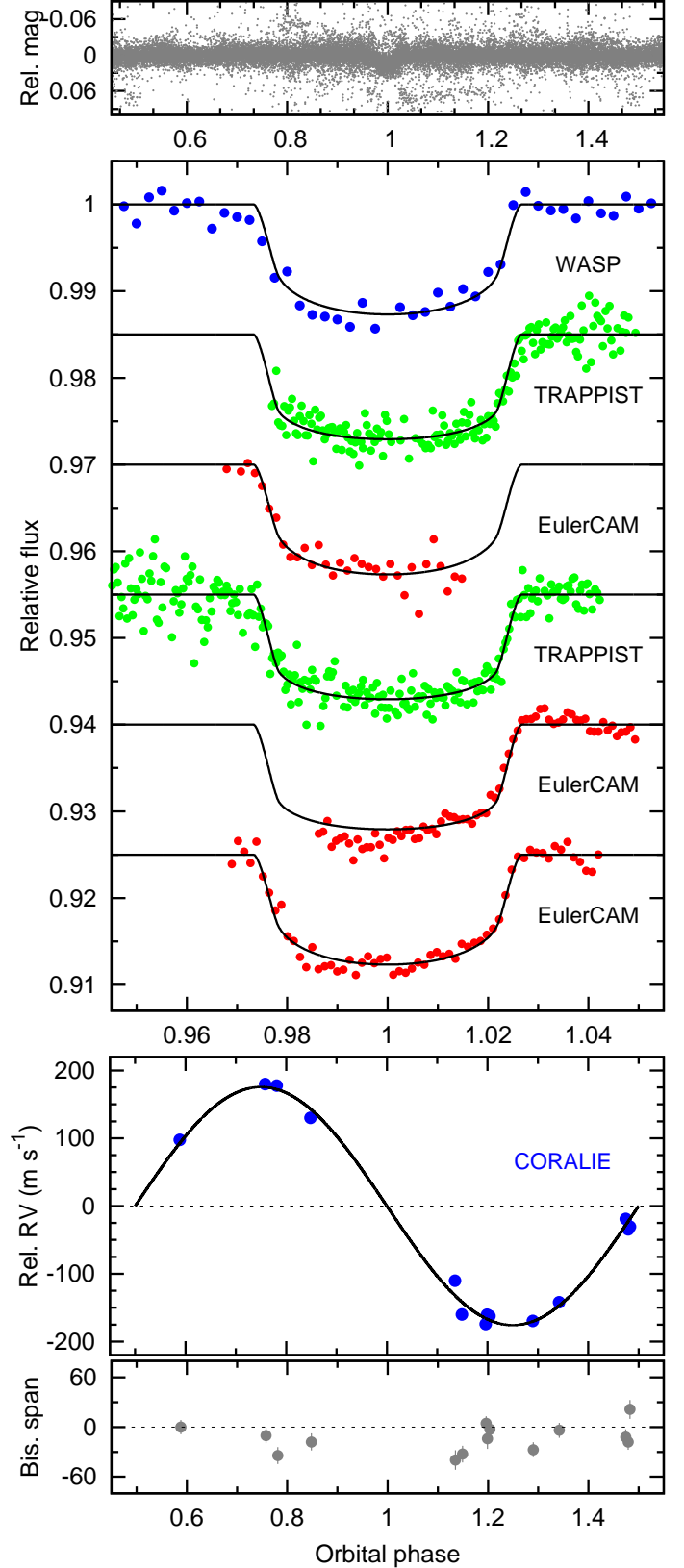
Figure 1. WASP-95b discovery data: (Top) The WASP data folded on the transit period. (Second panel) The binned WASP data with (offset) the follow-up transit lightcurves (ordered from the top as in Table 1) together with the fitted MCMC model. (Third) The CORALIE radial velocities with the fitted model. (Lowest) The bisector spans; the absence of any correlation with radial velocity is a check against transit mimics.

Table 3. System parameters for WASP-96.

1SWASP J000411.14–472138.2	
2MASS 00041112–4721382	
RA = $00^h04^m11.14^s$, Dec = $-47°21'38.2''$ (J2000)	
V mag = 12.2	
Rotational modulation < 1 mmag (95%)	
pm (RA) 23.1 ± 1.0 (Dec) 3.7 ± 1.0 mas/yr	

Stellar parameters from spectroscopic analysis.

Spectral type	G8
T_{eff} (K)	5500 ± 150
$\log g$	4.25 ± 0.15
$v \sin I$ (km s^{-1})	1.5 ± 1.3
[Fe/H]	$+0.14 \pm 0.19$
$\log A(Li)$	1.48 ± 0.15
Age (Lithium) [Gy]	$2 \sim 5$
Age (Gyro) [Gy]	8^{+26}_{-8}

Parameters from MCMC analysis.

P (d)	3.4252602 ± 0.0000027
T_c (HJD) (UTC)	$245\,6258.0621 \pm 0.0002$
T_{14} (d)	0.1011 ± 0.0011
$T_{12} = T_{34}$ (d)	0.0200 ± 0.0014
$\Delta F = R_P^2/R_*^2$	0.0138 ± 0.0003
b	0.710 ± 0.019
i (°)	85.6 ± 0.2
K_1 (km s^{-1})	0.062 ± 0.004
γ (km s^{-1})	-1.23300 ± 0.00009
e	0 (adopted) (< 0.27 at 3σ)
M_* (M$_\odot$)	1.06 ± 0.09
R_* (R$_\odot$)	1.05 ± 0.05
$\log g_*$ (cgs)	4.42 ± 0.02
ρ_* ($\rho_\odot$)	0.922 ± 0.073
T_{eff} (K)	5540 ± 140
M_P (M$_{Jup}$)	0.48 ± 0.03
R_P (R$_{Jup}$)	1.20 ± 0.06
$\log g_P$ (cgs)	2.88 ± 0.04
ρ_P (ρ_J)	0.28 ± 0.04
a (AU)	0.0453 ± 0.0013
$T_{P,A=0}$ (K)	1285 ± 40

Errors are 1σ; Limb-darkening coefficients were:
(Euler r) a1 = 0.722, a2 = –0.581, a3 = 1.203, a4 = –0.561
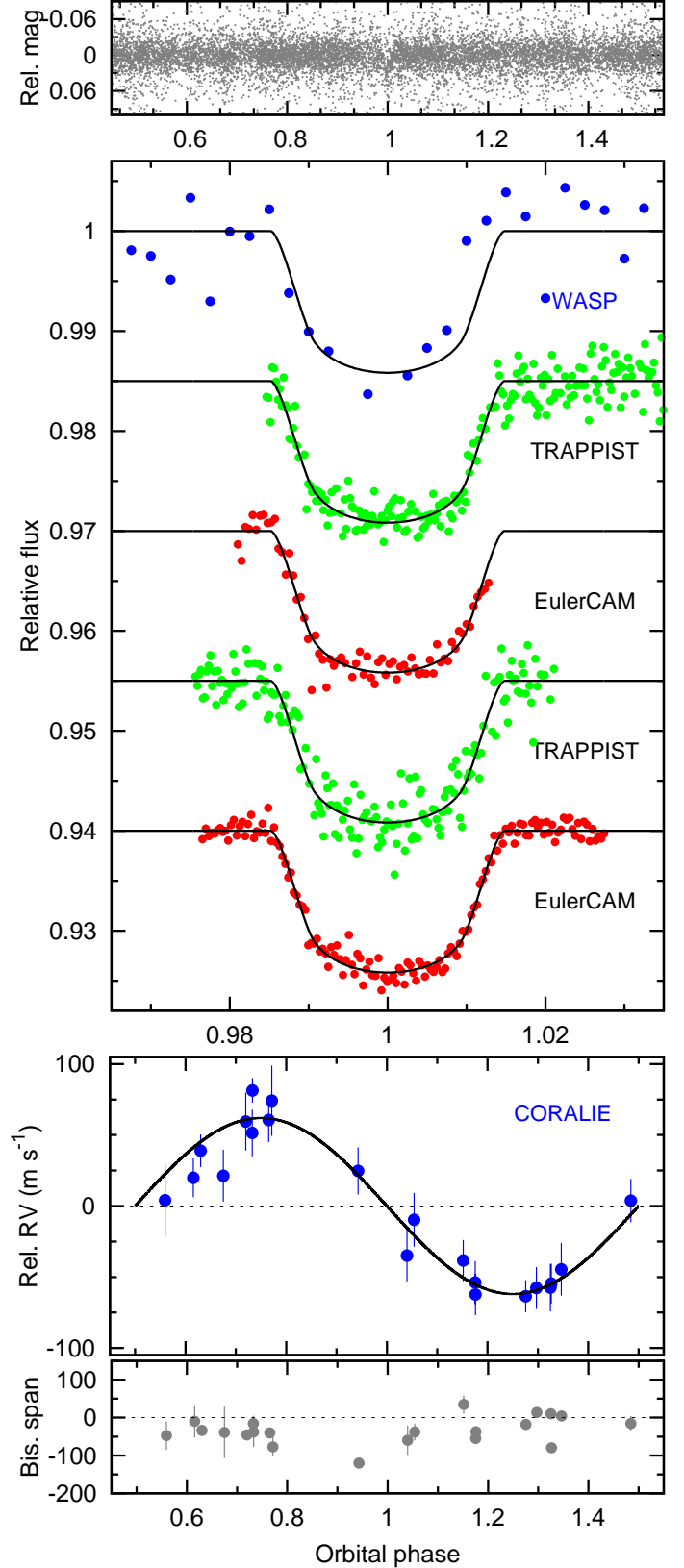(Trap BB) a1 = 0.722, a2 = –0.581, a3 = 1.203, a4 = –0.561

Figure 2. WASP-96b discovery data (as in Fig. 1).

Table 4. System parameters for WASP-97.

1SWASP J013825.04–554619.4
2MASS 01382504–5546194
RA = $01^h 38^m 25.04^s$, Dec = –55°46'19.4'' (J2000)
V mag = 10.6
Rotational modulation < 1 mmag (95%)
pm (RA) 94.6 ± 1.1 (Dec) 20.8 ± 1.0 mas/yr

Stellar parameters from spectroscopic analysis.

Spectral type	G5
T_{eff} (K)	5670 ± 110
$\log g$	4.45 ± 0.08
$v \sin I$ (km s^{-1})	1.1 ± 0.5
[Fe/H]	$+0.23 \pm 0.11$
log A(Li)	< 0.85
Age (Lithium) [Gy]	> 5
Age (Gyro) [Gy]	$11.9^{+16.0}_{-8.3}$

Parameters from MCMC analysis.

P (d)	2.072760 ± 0.000001
T_{c} (HJD) (UTC)	$245\,6438.18683 \pm 0.00018$
T_{14} (d)	0.1076 ± 0.0008
$T_{12} = T_{34}$ (d)	0.011 ± 0.001
$\Delta F = R_{\mathrm{P}}^2 / R_*^2$	0.0119 ± 0.0002
b	$0.23^{+0.11}_{-0.15}$
i (°)	$88.0^{+1.3}_{-1.0}$
K_1 (km s^{-1})	0.1945 ± 0.0023
γ (km s^{-1})	6.80877 ± 0.00029
e	0 (adopted) (< 0.05 at 3σ)
M_* (M$_\odot$)	1.12 ± 0.06
R_* (R$_\odot$)	1.06 ± 0.04
$\log g_*$ (cgs)	4.43 ± 0.03
ρ_* ($\rho_\odot$)	0.93 ± 0.09
T_{eff} (K)	5640 ± 100
M_{P} (M$_{\mathrm{Jup}}$)	1.32 ± 0.05
R_{P} (R$_{\mathrm{Jup}}$)	1.13 ± 0.06
$\log g_{\mathrm{P}}$ (cgs)	3.37 ± 0.04
ρ_{P} (ρ_{J})	0.91 ± 0.11
a (AU)	0.03303 ± 0.00056
$T_{\mathrm{P,A}=0}$ (K)	1555 ± 40

Errors are 1σ; Limb-darkening coefficients were:
(Euler r) a1 = 0.700, a2 = –0.489, a3 = 1.077, a4 = –0.516
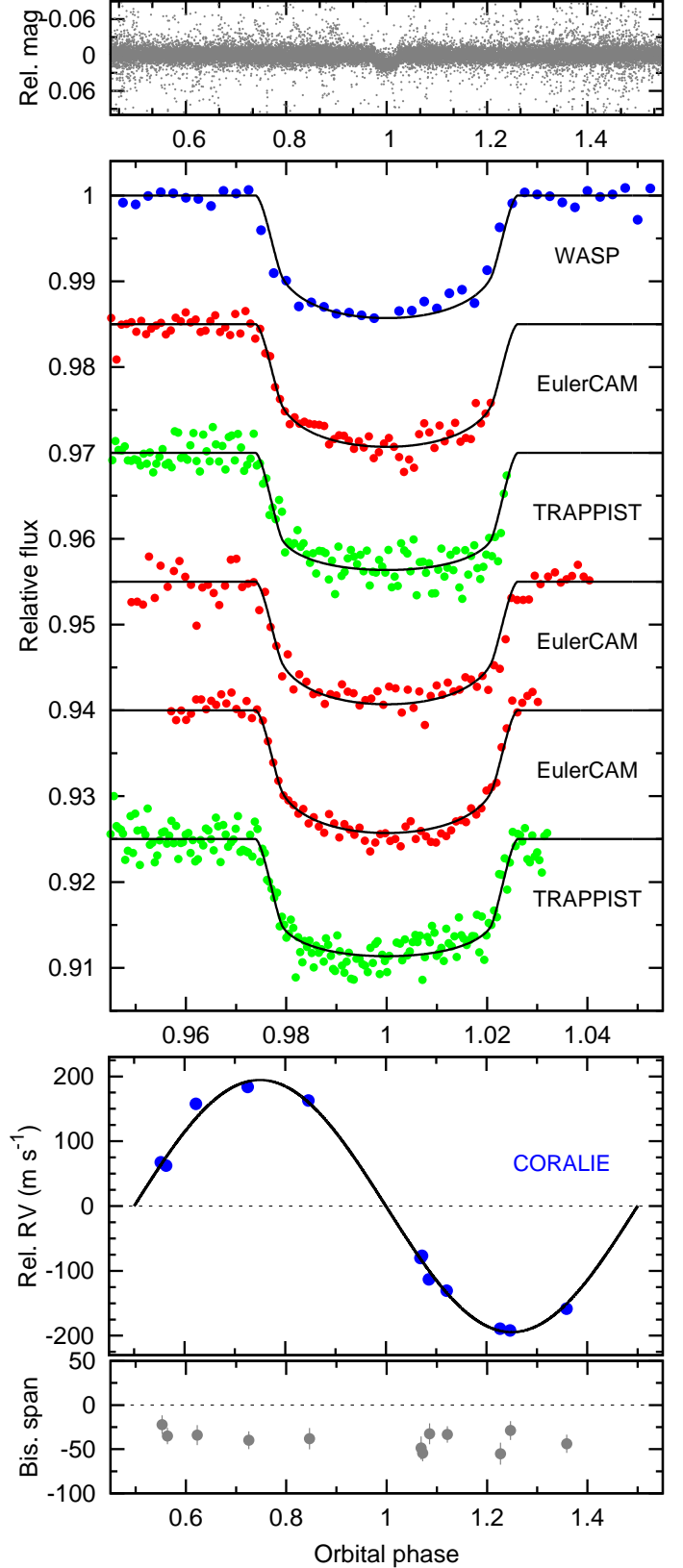(Trap Iz) a1 = 0.778, a2 = –0.713, a3 = 1.077, a4 = –0.484

Figure 3. WASP-97b discovery data (as in Fig. 1).

Table 5. System parameters for WASP-98.

1SWASP J035342.90–341941.7	
2MASS 03534291–3419414	
RA = $03^h 53^m 42.90^s$, Dec = –34°19′41.7″ (J2000)	
V mag = 13.0	
Rotational modulation < 2 mmag (95%)	
pm (RA) 32.0 ± 1.1 (Dec) -13.4 ± 1.1 mas/yr	

Stellar parameters from spectroscopic analysis.	
Spectral type	G7
$T_{\rm eff}$ (K)	5550 ± 140
$\log g$	4.40 ± 0.15
$v \sin I$ (km s^{-1})	< 0.5
[Fe/H]	-0.60 ± 0.19
log A(Li)	< 0.91
Age (Lithium) [Gy]	> 3
Age (Gyro) [Gy]	> 8

Parameters from MCMC analysis.	
P (d)	2.9626400 ± 0.0000013
$T_{\rm c}$ (HJD) (UTC)	$245\,6333.3913 \pm 0.0001$
T_{14} (d)	0.0795 ± 0.0005
$T_{12} = T_{34}$ (d)	0.0202 ± 0.0006
$\Delta F = R_{\rm P}^2 / R_*^2$	0.02570 ± 0.00025
b	0.71 ± 0.01
i (°)	86.3 ± 0.1
K_1 (km s^{-1})	0.15 ± 0.01
γ (km s^{-1})	-38.2882 ± 0.0003
e	0 (adopted) (< 0.24 at 3σ)
M_* (M$_\odot$)	0.69 ± 0.06
R_* (R$_\odot$)	0.70 ± 0.02
$\log g_*$ (cgs)	4.583 ± 0.014
ρ_* ($\rho_\odot$)	1.99 ± 0.07
$T_{\rm eff}$ (K)	5525 ± 130
$M_{\rm P}$ (M$_{\rm Jup}$)	0.83 ± 0.07
$R_{\rm P}$ (R$_{\rm Jup}$)	1.10 ± 0.04
$\log g_{\rm P}$ (cgs)	3.20 ± 0.03
$\rho_{\rm P}$ ($\rho_{\rm J}$)	0.63 ± 0.06
a (AU)	0.036 ± 0.001
$T_{\rm P, A=0}$ (K)	1180 ± 30

Errors are 1σ; Limb-darkening coefficients were:
(Euler *I*) a1 = 0.558, a2 = –0.157, a3 = 0.576, a4 = –0.325
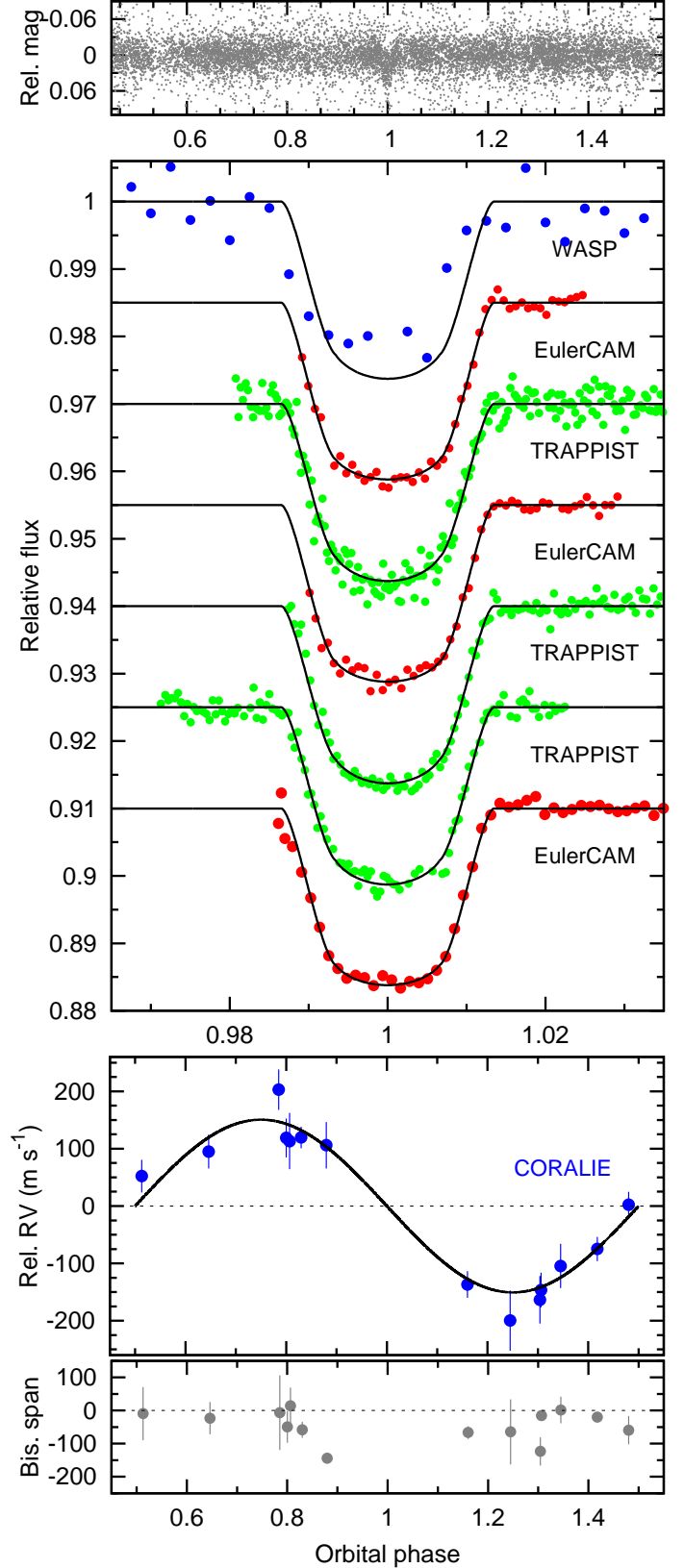(Trap BB) a1 = 0.486, a2 = 0.090, a3 = 0.444, a4 = –0.294

Figure 4. WASP-98b discovery data (as in Fig. 1).

Table 6. System parameters for WASP-99.

1SWASP J023935.44–500028.8
2MASS 02393544–5000288
RA = $02^h 39^m 35.44^s$, Dec = $-50°00'28.8''$ (J2000)
V mag = 9.5
Rotational modulation < 2 mmag (95%)
pm (RA) –2.7 ± 1.1 (Dec) –38.1 ± 0.9 mas/yr

Stellar parameters from spectroscopic analysis.

Spectral type	F8
$T_{\rm eff}$ (K)	6150 ± 100
$\log g$	4.3 ± 0.1
$v \sin I$ (km s^{-1})	6.8 ± 0.5
[Fe/H]	+0.21 ± 0.15
log A(Li)	2.52 ± 0.08
Age (Lithium) [Gy]	1 ∼ 3
Age (Gyro) [Gy]	$1.4^{+1.1}_{-0.6}$

Parameters from MCMC analysis.

P (d)	5.75251 ± 0.00004
$T_{\rm c}$ (HJD) (UTC)	245 6224.9824 ± 0.0014
T_{14} (d)	0.219 ± 0.003
$T_{12} = T_{34}$ (d)	$0.0137^{+0.0017}_{-0.0006}$
$\Delta F = R_{\rm P}^2/R_*^2$	0.0041 ± 0.0002
b	0.18 ± 0.17
i (°)	88.8 ± 1.1
K_1 (km s^{-1})	0.2422 ± 0.0017
γ (km s^{-1})	24.9610 ± 0.0002
e	0 (adopted) (< 0.02 at 3σ)
M_* (M$_\odot$)	1.48 ± 0.10
R_* (R$_\odot$)	$1.76^{+0.11}_{-0.06}$
$\log g_*$ (cgs)	$4.12^{+0.02}_{-0.04}$
ρ_* ($\rho_\odot$)	$0.27^{+0.02}_{-0.04}$
$T_{\rm eff}$ (K)	6180 ± 100
$M_{\rm P}$ (M$_{\rm Jup}$)	2.78 ± 0.13
$R_{\rm P}$ (R$_{\rm Jup}$)	$1.10^{+0.08}_{-0.05}$
$\log g_{\rm P}$ (cgs)	$3.72^{+0.03}_{-0.06}$
$\rho_{\rm P}$ ($\rho_{\rm J}$)	2.1 ± 0.3
a (AU)	0.0717 ± 0.0016
$T_{\rm P,A=0}$ (K)	1480 ± 40

Errors are 1σ; Limb-darkening coefficients were:
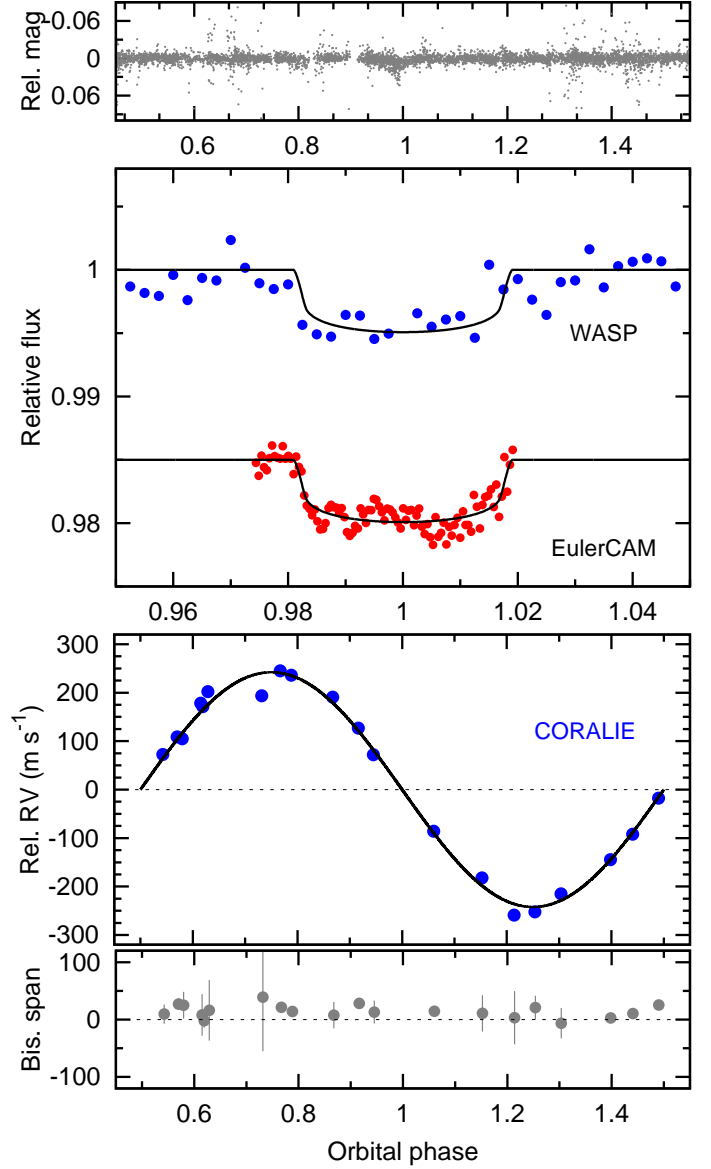(Euler r) a1 = 0.590, a2 = 0.036, a3 = 0.306, a4 = –0.205

Figure 5. WASP-99b discovery data (as in Fig. 1).

Table 7. System parameters for WASP-100.

1SWASP J043550.32–640137.3
2MASS 04355033–6401373
RA = $04^h35^m50.32^s$, Dec = $-64°01'37.3''$ (J2000)
V mag = 10.8
Rotational modulation   < 1 mmag (95%)
pm (RA) 11.9 ± 1.0 (Dec) -2.2 ± 2.3 mas/yr

Stellar parameters from spectroscopic analysis.

Spectral type	F2
T_{eff} (K)	6900 ± 120
$\log g$	4.35 ± 0.17
$v \sin I$ (km s^{-1})	12.8 ± 0.8
[Fe/H]	-0.03 ± 0.10
$\log A(Li)$	< 1.80
Age (Lithium) [Gy]	too hot
Age (Gyro) [Gy]	too hot

Parameters from MCMC analysis.

P (d)	2.849375 ± 0.000008
T_c (HJD) (UTC)	$245\,6272.3395 \pm 0.0009$
T_{14} (d)	0.160 ± 0.005
$T_{12} = T_{34}$ (d)	0.021 ± 0.005
$\Delta F = R_P^2/R_*^2$	0.0076 ± 0.0005
b	$0.64\,^{+0.08}_{-0.16}$
i (°)	$82.6\,^{+2.6}_{-1.7}$
K_1 (km s^{-1})	0.213 ± 0.008
γ (km s^{-1})	29.9650 ± 0.0002
e	0 (adopted) (< 0.10 at 3σ)
M_* (M$_\odot$)	1.57 ± 0.10
R_* (R$_\odot$)	2.0 ± 0.3
$\log g_*$ (cgs)	4.04 ± 0.11
ρ_* ($\rho_\odot$)	$0.20\,^{+0.10}_{-0.05}$
T_{eff} (K)	6900 ± 120
M_P (M$_{Jup}$)	2.03 ± 0.12
R_P (R$_{Jup}$)	1.69 ± 0.29
$\log g_P$ (cgs)	3.21 ± 0.15
ρ_P (ρ_J)	0.4 ± 0.2
a (AU)	0.0457 ± 0.0010
$T_{P,A=0}$ (K)	2190 ± 140

Errors are 1σ; Limb-darkening coefficients were:
(Trap Iz) a1 = 0.542, a2 = 0.086, a3 = 0.001, a4 = −0.055
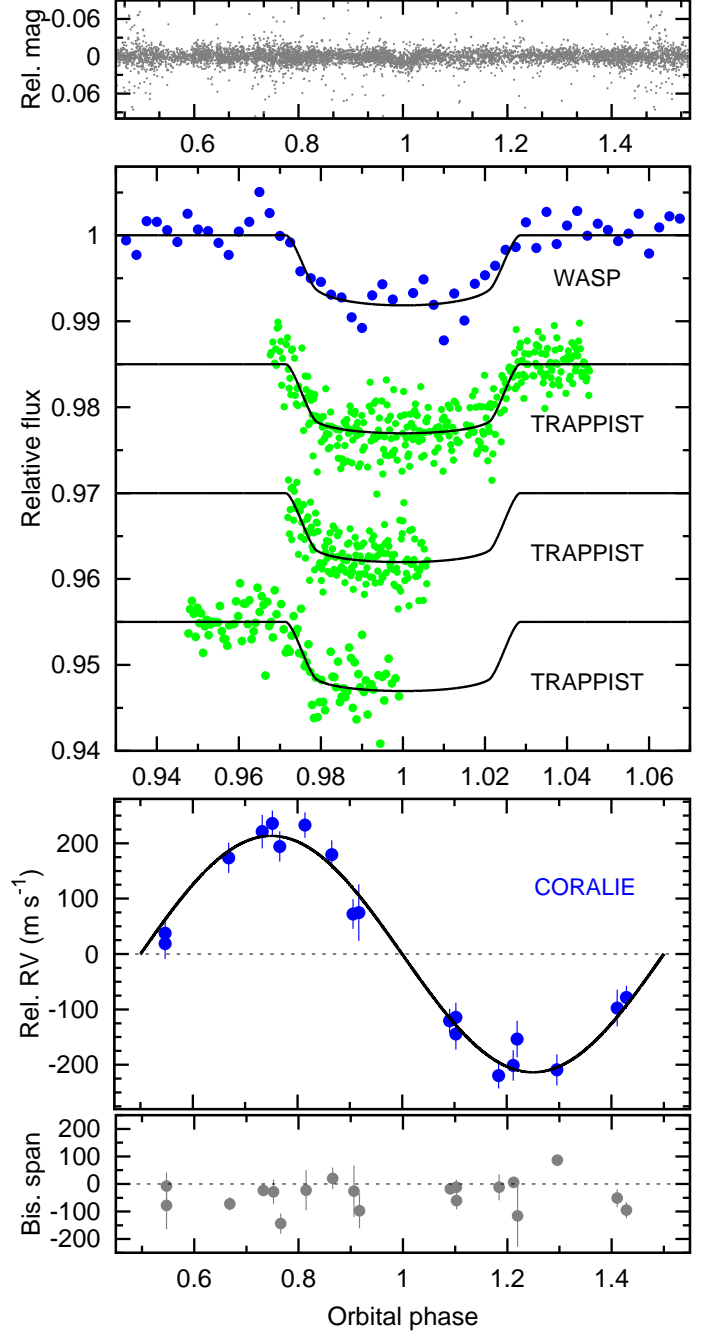
Figure 6. WASP-100b discovery data (as in Fig. 1).

Table 8. System parameters for WASP-101.

1SWASP J063324.26–232910.2
2MASS 06332426–2329103
RA = $06^h 33^m 24.26^s$, Dec = $-23°29'10.2''$ (J2000)
V mag = 10.3
Rotational modulation   < 1 mmag (95%)
pm (RA) -2.3 ± 0.9 (Dec) 23.3 ± 1.2 mas/yr

Stellar parameters from spectroscopic analysis.

Spectral type	F6
T_{eff} (K)	6380 ± 120
$\log g$	4.31 ± 0.08
$v \sin I$ (km s^{-1})	12.4 ± 0.5
[Fe/H]	$+0.20 \pm 0.12$
$\log A(\mathrm{Li})$	2.80 ± 0.09
Age (Lithium) [Gy]	$0.5 \sim 2$
Age (Gyro) [Gy]	$0.9^{+1.3}_{-0.4}$

Parameters from MCMC analysis.

P (d)	3.585722 ± 0.000004
T_c (HJD) (UTC)	2456164.6934 ± 0.0002
T_{14} (d)	0.113 ± 0.001
$T_{12} = T_{34}$ (d)	0.023 ± 0.001
$\Delta F = R_P^2 / R_*^2$	0.0126 ± 0.0002
b	0.736 ± 0.013
i (°)	85.0 ± 0.2
K_1 (km s^{-1})	0.054 ± 0.004
γ (km s^{-1})	42.6373 ± 0.0006
e	0 (adopted) (< 0.03 at 3σ)
M_* (M$_\odot$)	1.34 ± 0.07
R_* (R$_\odot$)	1.29 ± 0.04
$\log g_*$ (cgs)	4.345 ± 0.019
ρ_* ($\rho_\odot$)	0.626 ± 0.043
T_{eff} (K)	6400 ± 110
M_P (M$_{\mathrm{Jup}}$)	0.50 ± 0.04
R_P (R$_{\mathrm{Jup}}$)	1.41 ± 0.05
$\log g_P$ (cgs)	2.76 ± 0.04
ρ_P (ρ_J)	0.18 ± 0.02
a (AU)	0.0506 ± 0.0009
$T_{P,A=0}$ (K)	1560 ± 35

Errors are 1σ; Limb-darkening coefficients were:
(Trap z) a1 = 0.640, a2 = -0.172, a3 = 0.302, a4 = -0.174
(Euler r) a1 = 0.548, a2 = 0.238, a3 = -0.010, a4 = -0.067
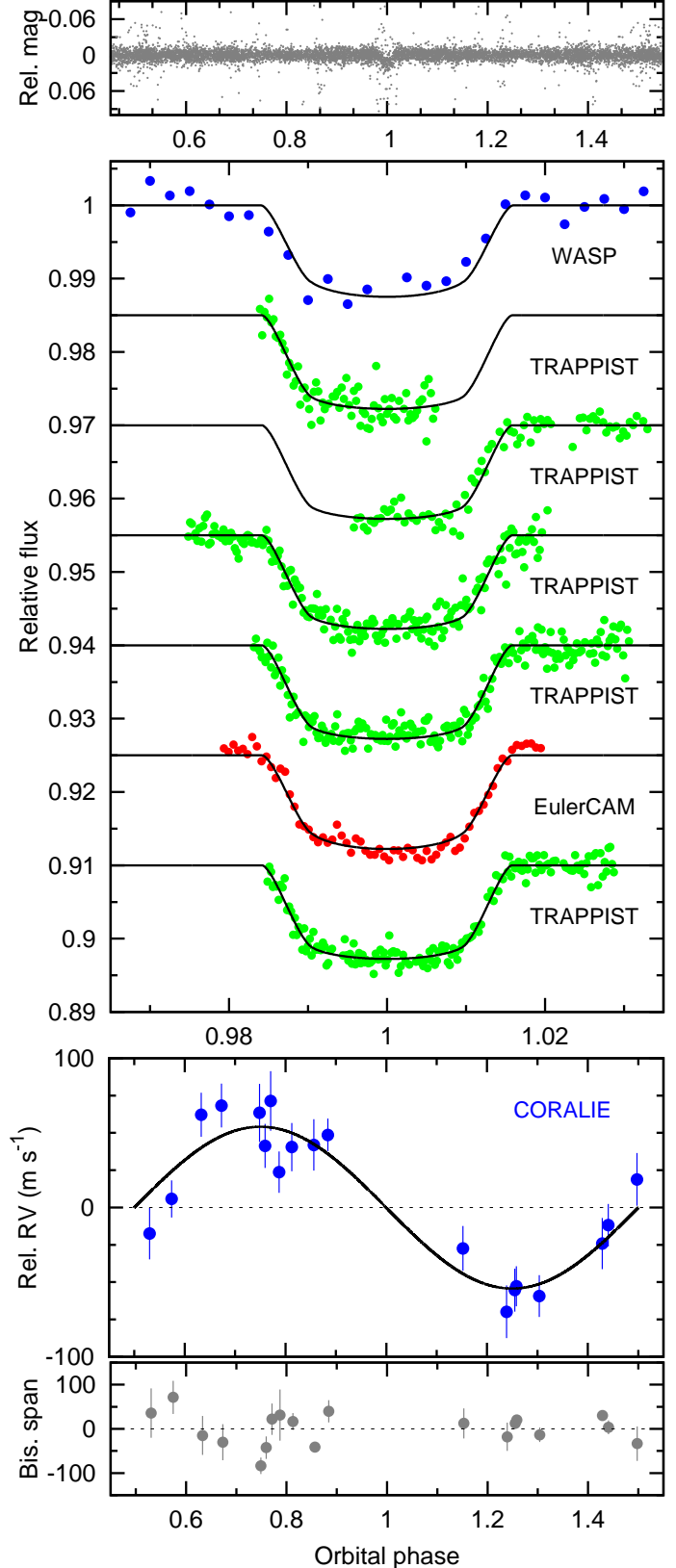
Figure 7. WASP-101b discovery data (as in Fig. 1).
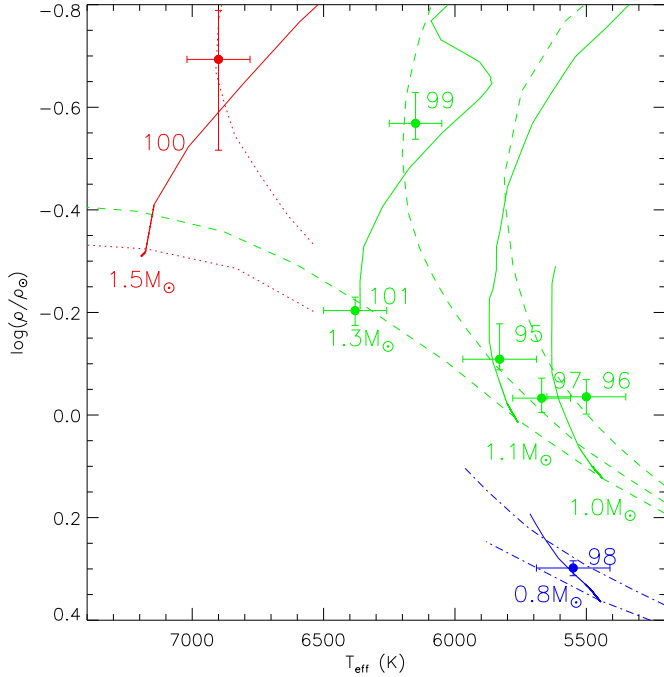
Figure 8. Evolutionary tracks on a modified H–R diagram ($\rho_*^{-1/3}$ versus $T_{\rm eff}$). The red lines are for solar metallicity, [Fe/H] = 0, showing (solid lines) mass tracks with the labelled mass, and (dashed lines) age tracks for log(age) = 7.85 & 9.15 yrs. The green lines are the same but for a higher metallicity of [Fe/H] = +0.19 and log(age) = 7.85, 9.4 & 9.8. The blue lines are the same for a lower metallicity of [Fe/H] = –0.6, and log(age) = 7.85 & 9.8 yrs. Stars are colour coded to the nearest of these metallicites. The models are from Girardi et al. (2000).

The fitted parameters were $T_{\rm c}$, P, ΔF, T_{14}, b, K_1, where $T_{\rm c}$ is the epoch of mid-transit, P is the orbital period, ΔF is the fractional flux-deficit that would be observed during transit in the absence of limb-darkening, T_{14} is the total transit duration (from first to fourth contact), b is the impact parameter of the planet's path across the stellar disc, and K_1 is the stellar reflex velocity semi-amplitude.

The transit lightcurves lead directly to stellar density but one additional constraint is required to obtain stellar masses and radii, and hence full parametrisation of the system. Here we use the calibrations presented by Southworth (2011), based on masses and radii of eclipsing binaries.

For each system we list the resulting parameters in Tables 2 to 8, and plot the resulting data and models in Figures 1 to 7. We also refer the reader to Smith et al. (2012) who present an extensive analysis of the effect of red noise in the transit lightcurves on the resulting system parameters.

As in past WASP papers we plot the spectroscopic $T_{\rm eff}$, and the stellar density from fitting the transit, against the evolutionary tracks from Girardi et al. (2000), as shown in Fig. 8.
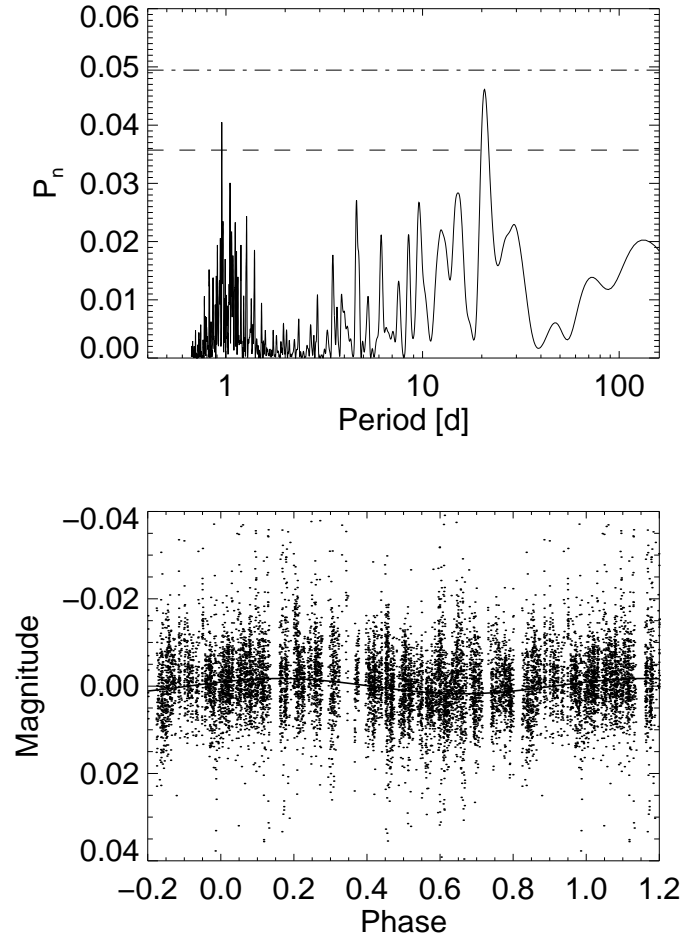

Figure 9. The possible rotational modulation in WASP-95 at a period of 20.7 d. The horizontal lines are the 10% (dashed) and 1% (dot-dashed) false-alarm probabilities. The upper plot is the periodogram (the y-scale being the fraction of the scatter in the data that is modelled by a sinusoidal variation, weighted by the standard errors); the lower plot is the data folded on the 20.7-d period.

4.1   WASP-95

WASP-95 is a $V = 10.1$, G2 star with an [Fe/H] of $+0.14 \pm 0.16$. It may be slightly evolved, with an age of several billion years.

WASP-95 shows a possible rotational modulation at a period of 20.7 d and an amplitude of 2 mmag in the WASP data (Fig. 9), though this is seen in only one of the two years of data. The values of $v \sin i$ from the spectroscopic analysis (assuming that the spin axis is perpendicular to us) and the stellar radius from the transit analysis combine to a rotation period of 19.7 ± 3.9 d, which is compatible with the possible rotational modulation.

WASP-95b is a typical hot Jupiter ($P_{\rm orb} = 2.18$ d, $M = 1.2$ $M_{\rm Jup}$, $R = 1.2$ $R_{\rm Jup}$).

4.2 WASP-96

WASP-96 is fainter G8 star, at $V = 12.2$, with an [Fe/H] of $+0.14 \pm 0.19$. The planet is a typical hot Jupiter ($P_{orb} = 3.4$ d, $M = 0.5$ M$_{Jup}$, $R = 1.2$ R$_{Jup}$).

4.3 WASP-97

WASP-97 is a $V = 10.6$, G5 star, with an above-solar metallicity of [Fe/H] of $+0.23 \pm 0.11$. The planet is again a typical hot Jupiter ($P_{orb} = 2.1$ d, $M = 1.3$ M$_{Jup}$, $R = 1.1$ R$_{Jup}$).

4.4 WASP-98

At $V = 13.0$, WASP-98 is at the faint end of the WASP-South/CORALIE survey. The spectral analysis has a lower S/N of only 40 and so is less reliable. It appears to be exceptionally metal poor ([Fe/H] = -0.6 ± 0.19) for a transit host star. The spectral analysis suggests G7, though the transit parameters lead to a lower mass of 0.7 M$_\odot$. The planet is a typical hot Jupiter having a high-impact ($b = 0.7$) transit.

4.5 WASP-99

WASP-99 is the brightest host star reported here, at $V = 9.5$. Spectral analysis suggests that it is an F8 star with [Fe/H] of $+0.21 \pm 0.15$, though the transit analysis gives a higher mass ($M = 1.5$ M$_\odot$) and an expanded radius ($R = 1.8$ R$_\odot$). The planet is relatively massive ($M = 2.8$ M$_{Jup}$), though its mass and radius are similar to those of many known planets.

The transit of WASP-99b is the shallowest yet found by WASP-South, at 0.0041 ± 0.0002, along with that of WASP-72b at 0.0043 ± 0.0004 (Gillon et al. 2013).

4.6 WASP-100

WASP-100 is a $V = 10.8$, F2 star of solar metallicity. The planet is a typical bloated hot Jupiter ($P_{orb} = 2.8$ d, $M = 2.0$ M$_{Jup}$, $R = 1.7$ R$_{Jup}$) with a high irradiation (see, e.g., West et al. 2013).

4.7 WASP-101

WASP-101 is a $V = 10.3$, F6 star with [Fe/H] = $+0.20 \pm 0.12$. The analysis is compatible with an unevolved main-sequence star. The planet is a bloated, low-mass planet ($P_{orb} = 3.6$ d, $M = 0.50$ M$_{Jup}$, $R = 1.4$ R$_{Jup}$).

5 COMPLETENESS

With the WASP survey now passing WASP-100 we can ask how complete the survey methods are and how many planets we are missing. A full discussion of selection effects is a large topic and is not attempted here, but we can use the HAT project as a straightforward check on our techniques. The HAT project (Bakos et al. 2004) is very similar in conception and hardware to WASP, and thus whether a HAT planet is also detected by us gives an indication of how many we are overlooking.
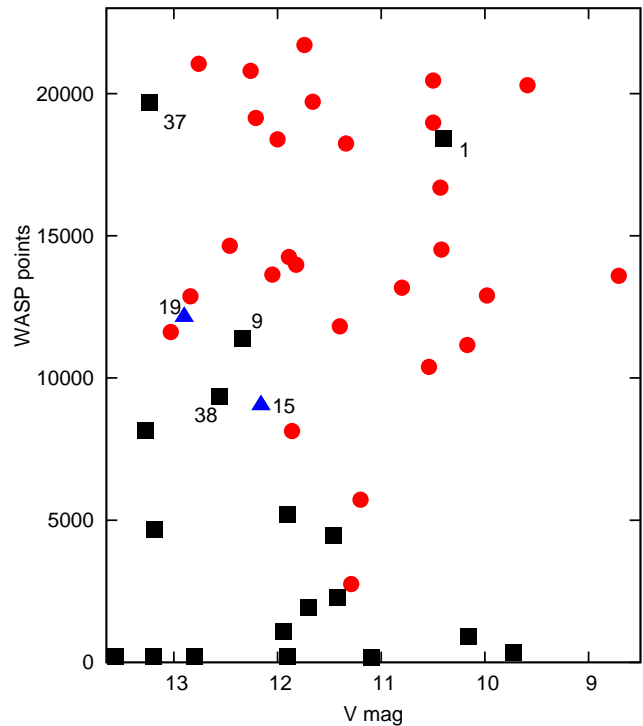
Figure 10. The number of WASP data points on each HAT planet as a function of magnitude. Red circles denote that the planet is detected by WASP, blue triangles are marginal detections, black squares are non-detections. Some planets are labelled by their HAT number.

Fig. 11 shows, for each HAT planet (up to HAT-P-46 and HATS-3b), the number of data points it has in the WASP survey and whether we also detect it. There is some level of subjectivity in claiming a detection, since all WASP candidates are scrutinised by eye, and thus two planets are shown as marginal detections. Most non-detections result from there being little or no WASP data (< 6000 data points), but it is worthwhile to review the remaining 7 cases.

HAT-P-1 (Bakos et al. 2007) is bright and has 14 000 points in WASP data. It isn't detected owing to some excess noise in some parts of our automated photometry, which prevents the transit-search algorithm from finding the transits. HAT-P-9b (Shporer et al. 2009) has $V = 12.3$ and there are 11 000 WASP points. There is excess noise in some of the WASP photometry, preventing the search algorithm finding the transit. These two are the worst failures of the WASP techniques applied to the HAT sample.

HAT-P-37 (Bakos et al. 2012) at $V = 13.2$ is fainter than any WASP planet, and also has a brighter eclipsing binary 68" away, which misleads the WASP search algorithms. HAT-P-38 (Sato et al. 2012) is relatively faint ($V = 12.6$) and there is relatively limited WASP data (9000 points).

Of the two marginal detections, HAT-P-19b (Hartman et al. 2011) has 12 000 WASP points but is faint ($V = 12.9$) and has an orbital period of 4.008 d. As a single-longitude survey, WASP's sampling hampers the finding of integer-day periods. HAT-P-15b (Kovács et al. 2010) is also below 12th magnitude ($V = 12.2$), and has relatively sparse coverage

by WASP (9000 points), and also has a long orbital of 10.86 d, giving fewer transits than the typical 2–5-d hot Jupiters.

Thus, in summary, at brighter than $V = 12.8$ and given 10 000 WASP points (roughly two seasons of data) we fail to detect only 2 out of 23 HAT-discovered planets (note that the number 23 doesn't include independent discoveries by HAT of WASP planets). Thus we conclude that, in well-covered regions of sky, the WASP-South survey techniques give fairly complete discoveries for the sort of planets findable by WASP-like surveys. That means hot Jupiters around stars in the magnitude range $V = 9$–13, and excluding crowded areas of sky such as the galactic plane. It also applies only to stars later than mid F, since hotter stars don't give good RV signals.

The lower period limit of 0.8 d is likely a real cut-off in the distribution of hot Jupiters (e.g., Hellier et al. 2011), since we routinely look for candidates down to periods of 0.5 d. The longer period limit is primarily set by the amount of observational coverage, and our completeness will drop off above $P_{\rm orb} \sim 7$ d, though this could increase to 'warm' Jupiters beyond ~ 10 d as WASP continues to accumulate data.

The upper limit in planetary size is also likely a real feature of hot Jupiters, given the number of systems found with $R = 1.8$–2.0 $R_{\rm Jup}$, but not above that range. The lower size limit of WASP discoveries is set primarily by red noise and so is harder to evaluate. Fig. 12 shows the transit depths of WASP planets, suggesting that we have a good discovery probability down to depths of $\sim 0.5\%$ in the magnitude range $V = 9$–12. This is sufficient for $R \gtrsim 0.9$ $R_{\rm Jup}$ given $R_* < 1.3$ $R_\odot$, and $\gtrsim 0.7$ $R_{\rm Jup}$ given < 1.0 $R_\odot$, and thus is sufficient for most hot Jupiters.

REFERENCES

Anderson D. R. et al., 2012, MNRAS, 422, 1988
Bakos G. À., Noyes R. W., Kovács G., Stanek K. Z., Sasselov, D. D., Domsa, I., 2004, PASP, 116, 266
Bakos, G. Á. et al., 2007, ApJ, 656, 552
Bakos, G. Á. et al., 2012, AJ, 144, 19
Barnes, S.A. 2007, ApJ, 669, 1167
Claret, A., 2000, A&A, 363, 1081
Collier Cameron, A., et al., 2007a, MNRAS, 375, 951
Collier Cameron, A., et al., 2007b, MNRAS, 380, 1230
Doyle, A.P. et al. 2013, MNRAS,, 428, 3164
Gillon, M., et al., 2013, A&A, 552, A82
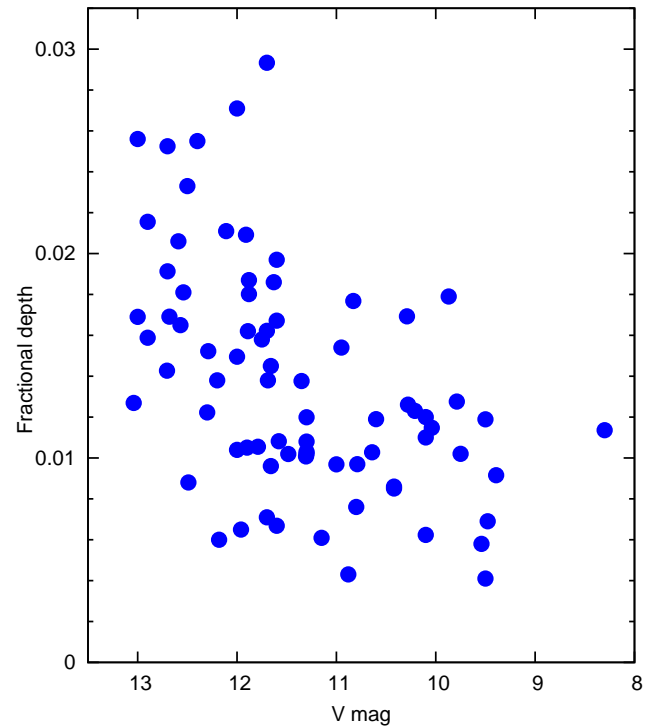Girardi, L., Bressan, A., Bertelli, G., Chiosi, C. 2000, A&AS, 141, 371

Figure 11. The transits depths of WASP planets as a function of host-star magnitude.

Gray D.F., 2008, The observation and analysis of stellar photospheres, 3rd Edition (Cambridge University Press)
Hartman, J. D. et al., 2011, ApJ, 726, 52
Hellier, C. et al., 2012, MNRAS, 426, 739
Hellier, C. et al., 2011, A&A, 535, L7
Jehin, E. et al., 2011, Messenger, 145, 2
Kovács, G. et al., 2010, ApJ, 724, 866
Lendl, M. et al., 2012, A&A, 544, A72
Maxted, P.F.L. et al. 2011, PASP, 123, 547
Pollacco, D., et al., 2006, PASP, 118, 1407
Pollacco, D., et al., 2008, MNRAS, 385, 1576
Sato, B. et al., 2012, PASJ, 64, 97
Sestito, P. & Randlich, S., 2005, A&A, 442, 615
Shporer, A., et al., 2009, ApJ, 690, 1393
Smith A. M. S. et al. 2012, AJ, 143, 81
Southworth J., 2011, MNRAS, 417, 2166
Zacharias, N., Finch, C. T., Girard, T. M., Henden, A., Bartlett, J. L., Monet, D. G., Zacharias, M. I. 2013, AJ, 145, 44
West, R. G. et al. 2013, A&A, submitted